

Anthropogenic Pu distribution in Tropical East Pacific

著者	Kinoshita Norikazu, Sumi Takahiro, Takimoto Kiyotaka, Nagaoka Mika, Yokoyama Akihiko, Nakanishi Takashi
journal or publication title	Science of the Total Environment
volume	409
number	10
page range	1889-1899
year	2011-04-15
URL	http://hdl.handle.net/2297/27311

doi: 10.1016/j.scitotenv.2011.01.047

Anthropogenic Pu distribution in Tropical East Pacific

Norikazu Kinoshita¹, Takahiro Sumi², Kiyotaka Takimoto², Mika Nagaoka², Akihiko Yokoyama³,
Takashi Nakanishi³

¹Research Facility Center for Science and Technology, University of Tsukuba,
1-1-1 Ten-nodai, Tsukuba, Ibaraki 305-8577, Japan.

²Graduate School of Natural Science and Technology, Kanazawa University,
Kakuma-machi, Kanazawa, Ishikawa 920-1192, Japan.

³Institute of Science and Engineering, Kanazawa University
Kakuma-machi, Kanazawa, Ishikawa 920-1192, Japan.

Corresponding Author:

Norikazu Kinoshita

1-1-1 Ten-nodai, Tsukuba, Ibaraki 305-8577, Japan.

Tel: +81-29-853-2498

E-mail: kinoshita@tac.tsukuba.ac.jp

Abstract

The geographical distribution of the anthropogenic radionuclides ^{238}Pu and $^{239+240}\text{Pu}$ in the Tropical East Pacific in 2003 was studied from the viewpoint of material migration. We measured the contents of Pu isotopes in seawater and in sediment from the sea bottom. The distributions of Pu isotopes, together with those of coexisting nitrate and phosphate species and dissolved oxygen, are discussed in relation to the potential temperature and potential density ($\sigma\text{-}\theta$). The Pu contents in sediment samples were compared with those in the seawater. Horizontal migration across the Equator from north to south was investigated at depths down to ~800 m in the eastern Pacific. The Pu distribution at 0–400 m correlated well with the distribution of potential temperature. Maximum Pu levels were observed in the subsurface layer at 600–800 m, corresponding to the depth where $\sigma\text{-}\theta \approx 27.0$. It is suggested that the Pu distribution depends on the structure of the water mass and the particular temperature and salinity. The water column/sediment column inventory ratio and the vertical distribution of Pu may reflect the efficiency of scavenging in the relevant water areas.

Key words

Plutonium isotopes

Sea water

Sea sediment

Geographical distribution

Tropical East Pacific

1. Introduction

Radionuclides emitted during atmospheric tests of nuclear weapons have been widely used as proxies for tracing the migrations of materials (Doney, 1992; Tosaki et al., 2007). Most of these nuclides were deposited on the oceans, which occupy about 70% of the Earth's surface. It is believed that nuclides present as insoluble species become adsorbed by suspended materials in seawater. The suspended materials, together with the radionuclides that they contain, subsequently sink from the surface to the sea bottom, whereas soluble species, such as ^{137}Cs , remain in the surface waters for many years (Yamada and Wang, 2007) and migrate both vertically and horizontally under the influence of oceanic currents.

All isotopes of Pu are artificial radioactive nuclides. Most of the isotopes [^{238}Pu ($T_{1/2} = 87.7$ yr), ^{239}Pu ($T_{1/2} = 2.411 \times 10^4$ yr), ^{240}Pu ($T_{1/2} = 6.563 \times 10^3$ yr), ^{241}Pu ($T_{1/2} = 14.254$ yr), ^{242}Pu ($T_{1/2} = 3.833 \times 10^5$ yr), and ^{244}Pu ($T_{1/2} = 8.08 \times 10^7$ yr)] that are found in the environment were discharged from above-ground tests of nuclear weapons during the 1950s and early 1960s (Perkins and Thomas, 1980; Aarkrog, 2003). In addition, some Pu nuclides originate from various accidental releases and from reprocessing of nuclear materials (Kershaw et al., 1999).

Several investigations have been carried out by using environmental Pu isotopes. The chemical forms of Pu in seawater were evaluated by Aston (1980), who focused on its valence state and stability constant with inorganic ligands. The Pu nuclides in size-fractionated particles were analyzed by Dai et al. (2001), who reported that the most Pu exists in a low-molecular-weight fraction, with a few percent of Pu in a colloidal form. Several researchers have measured the atom ratios of Pu isotopes in sea sediment and in the ferromanganese crust by means of accelerator mass spectrometry (Paul et al., 2001; Wallner et al., 2000). Pu isotopes of mass numbers up to 244, formed a result of multiple neutron capture by ^{239}Pu , have been measured. In addition, several researchers have measured Pu concentrations and $^{240}\text{Pu}/^{239}\text{Pu}$ atom ratios in seawater, sediment, and land soil (Buesseler and Sholkovitz, 1987; Buesseler, 1997; Cooper et al., 2000; Kelley et al., 1999).

Seawater and sediment from the North Pacific exhibited a wide range of $^{240}\text{Pu}/^{239}\text{Pu}$ ratios (0.19–0.34), and higher ratios tended to be found near the sites of nuclear tests. In terms of the vertical distribution in seawater, the concentration of $^{239+240}\text{Pu}$ is generally low in surface waters, increases to a maximum at 500–1000 m, and then decreases in deeper waters. Vertical and horizontal distributions, including the GEOSECS data, have also been reported elsewhere (Bowen et al., 1980; Livingston et al., 2001). Lee et al. (2005) reported $^{239+240}\text{Pu}$ activities in sea sediments. A computer simulation of the scavenging and fate of Pu isotopes in seawater was carried out by Perriñez (1998).

In addition to the ^{238}Pu released from nuclear tests and by accident, additional ^{238}Pu was released when the Transit-5BN-3 navigation satellite, powered by a SNAP-9a nuclear generator fuelled with ^{238}Pu , failed to achieve orbit and burnt up on reentry at an altitude of about 50 km over the Indian Ocean in 1964. In the Northern Hemisphere, the estimated release of ^{238}Pu was 230 TBq from nuclear tests and 110 TBq from SNAP-9a; the corresponding figures for the Southern Hemisphere were 59 TBq and 380 TBq, respectively (Harley, 1980). The ratio of ^{238}Pu inventory released by nuclear testing to that released from SNAP-9a is estimated to be 2.0 in the Northern Hemisphere and 0.16 in the Southern Hemisphere.

In the East Pacific, there is an oceanic ridge, named the East Pacific Rise, an upwelling region and also high nutrient low chlorophyll region resulting from the poverty of iron. Variations in climatic conditions such as surface temperature occur in the Equatorial Pacific because of the El Niño Southern Oscillation (Tourigny and Jones, 2009). On the other hand, horizontal migration should be uncomplicated because there are few islands to block the oceanic currents. The North Equatorial Current, North Pacific Current, Equatorial Counter Current, South Equatorial Current, California Current, and Peru Current are of importance for surface migration in the Tropical East Pacific.

It was of interest, therefore, to determine how Pu is distributed in the East Pacific, given

the conditions mentioned above. If levels of isotopes in a variety of water-mass structures over an extensive region could be compared with each other and with previously reported levels, and if they could be correlated with levels of dissolved oxygen, water temperatures, and water densities, we might be able to understand which parameters affect the migration and distribution of Pu. Here, we report the vertical and horizontal distributions of ^{238}Pu and $^{239+240}\text{Pu}$ activities as well as the Pu inventory present in samples of seawater and sediment collected in the Tropical East Pacific during 2003, and we discuss our results in relation to material migration in seawater.

2. Experimental

2.1. Sampling

Samples of seawater and sediment from the Tropical East Pacific were collected during the KH-03-1 “Hydra” expedition of the *R/V Hakuho-Maru* in 2003. The locations of the sampling stations, the water depths, and the sampling dates are listed in Table 1, and the locations are shown in Fig. 1. Large-volume water samples (250 L) were collected at various depths between the surface and the bottom by using acoustically triggered quadruple PVC sampling bottles. Additionally, samples of sea sediment with diameter of 7 cm from the surface of the sea bottom to a depth of about 30 cm below the sea bottom were taken by using a multiple corer at locations HY-1, HY-2, HY-3, HY-6, and HY-9. The sediment cores were sliced into 1-cm-thick pieces. Additional samples of seawater (12 L) were collected by using a CTD Carousel multi-sampling (CTD-CMS) system fitted with a dissolved-oxygen (DO) sensor. The water pressure, water temperature, salinity, and DO were measured by devices incorporated into the CTD-CMS. In addition, small portions of seawater samples collected with the CTD-CMS were subjected to analysis for salinity, DO, nitrate, silicate, phosphate, etc.

2.2. Analysis of sea water

Unfiltered seawater samples (~250 L) were acidified with HCl to a pH of less than 1.5 and spiked with ^{242}Pu tracer and Fe^{3+} carrier. The solution was left to stand for more than 24 h to ensure chemical equilibration, then neutralized with aqueous ammonia to coprecipitate Pu with $\text{Fe}(\text{OH})_3$. The precipitate was separated from the solution and brought back to Japan for subsequent chemical analysis.

The Pu isotopes were analyzed by a procedure similar to that described by Kinoshita et al. (2007). Most of iron atoms were removed from the solution by solvent extraction with diisopropyl ether, and the remaining iron and Pu atoms were precipitated with aqueous ammonia. The precipitate was dissolved in 8 M HNO_3 , and reduced with NaNO_2 to ensure that all the Pu was in the Pu(IV) oxidation state. The solution was then passed through an anion-exchange column of Dowex 1X8, (100–200 mesh), and Th ions were eluted with 8 M HCl. Pu ions were subsequently eluted with 8 M HCl–0.1 M HI solution. This column separation was repeated to purify the resulting Pu solution. The Pu solution was then evaporated to dryness and the residue was dissolved in aqueous ammonium sulfate. The resulting solution was used to prepare an electrodeposited sample on a stainless-steel disk for assay by alpha spectrometry. The typical chemical efficiency of the entire procedure was 50%

2.3. Analysis of sea sediment

Dried sea sediment was mixed with four times its weight of solid NaOH, transferred to a Ni crucible, spiked with ^{242}Pu , and digested for ~12 h at 400 °C. The residue was dissolved in concentrated HCl, and iron atoms were removed by extraction with diisopropyl ether. The resulting sample was subjected to the same column separation and alpha spectrometry procedure as described above in Section 2.2.

3. Hydrography

The sampling stations HY-1 and HY-2 are located in the North Subtropical Gyre, whereas HY-11, HY-12, HY-15A, HY-17, and HY-18 are in the South Subtropical Gyre. Stations HY-6, HY-9, and HY-11 are located in the Peru Current. Station HY-6 is located in the terminal area of the Equatorial Undercurrent and, therefore, in the upwelling of the current, which is related to El Niño. El Niño was observed in 2002 to 2003 (Lagerloef et al., 2003). The potential temperature–salinity (θ – S) diagrams for the HY stations are shown in Fig. 2. The θ – S diagrams show various features near the surface where the potential temperature is above 15 °C. In particular, a low salinity related to the California Current, which includes land water, was observed at the surface at station HY-3, but not at HY-1 or HY-2. Similar profiles were observed below 12 °C at stations HY-3, HY-6, HY-9, and HY-11. Antarctic Intermediate Water (AAIW), characterized by a minimum salinity (practical salinity scale) of 34.3 at a potential temperature of 5 °C, appears at approximately 800 m at stations HY-15A, HY-17, and HY-18. It was reported that AAIW was observed on the WOCE P13 survey at 12° N on the 165° E line in 1992 (Kawabe and Taira, 1998). A tropical thermocline dome (the Costa Rica Dome) has been observed several times at around 9° N 90° W (Fiedler, 2002).

4. Result

The contents of ^{238}Pu and $^{239+240}\text{Pu}$ were deduced from the count rates of plutonium isotopes, including a yield tracer of ^{242}Pu , as measured by alpha spectrometry. Because the energies of alpha rays from ^{239}Pu and ^{240}Pu are too close to be distinguished from one another, we determined the sum of the activities $^{239+240}\text{Pu}$. Vertical profiles of ^{238}Pu and $^{239+240}\text{Pu}$ in seawater are listed in Table 2 and shown in Fig. 3. The potential temperature, salinity, potential density (σ - θ), and DO are also listed in Table 2. The Pu activities in sea sediment are listed Table 3 and shown in

Fig. 4. The standard uncertainty of the background count was used to estimate the detection limit. The activities of ^{238}Pu were too low to permit discussion of its vertical profile. Maxima in the $^{239+240}\text{Pu}$ activity were observed at around 500 m for HY-11, 800 m for HY-17 and HY-18, and 600 m for the other stations.

5. Discussion

5.1. Distribution of $^{239+240}\text{Pu}$ activity and the $^{238}\text{Pu}/^{239+240}\text{Pu}$ activity ratio in sea water

Figure 5 shows contour displays of the horizontal distribution of $^{239+240}\text{Pu}$ along the sailing course, as constructed by interpolation of the measured Pu concentrations. Table 4 lists the inventories of ^{238}Pu and $^{239+240}\text{Pu}$, derived by summing the activities at each station. According to UNSCEAR (2000), the total activities of fission products of Pu deposited in the Northern Hemisphere are reported to be 3–4 times greater than the corresponding values in the Southern Hemisphere. The inventories of $^{239+240}\text{Pu}$ at HY-1 to HY-3 were also 3–4 times higher than were those at HY-12 to HY-18, but almost same as those at HY-6 and HY-9. These anomalies at HY-6 to HY-11 are discussed below. The measured ratio of the Pu inventory in the Northern Hemisphere to that in the Southern Hemisphere corresponds with the previously reported ratio, except in the cases of stations HY-6 to HY-11.

Sano et al. (1995) discovered an extensive plume of water enriched in ^3He at a depth of about 2000 m in the South Pacific. This ^3He plume could be observed at distances of up to 5000 km west of the East Pacific Rise. In other words, a deep current flowing toward the west may be present in the South Central Pacific. We believe that horizontal migration of Pu at a depth of ~2000 m could be affected by this current. In addition, a pathway involving the North Pacific Tropical Water (NPTW) and North Pacific Intermediate Water (NPIW) has been discussed by Amakawa et al. (2009) and by You (2003). It has been reported that the NPTW and NPIW flow clockwise in the

North Pacific, so that a current is expected to flow from east to west in the region of HY-1 and HY-2. However, horizontal migration was not clearly demonstrated in our observations on Pu isotopes (Fig. 5).

On the assumption that the sinking behavior of Pu isotopes would result in a depth profile, the percentage of the $^{239+240}\text{Pu}$ inventory at each depth should reflect the rate of sinking. The results in Table 4 show that 30% of Pu was found in the layer between 0 and 1000 m at HY-9 and HY-11, whereas 40–50% of Pu was present at 0–1000 m at the other stations. If we compare results for similar longitudes, the percentages of Pu inventory in the 1000–2000 m layer at HY-17 and HY-18 are greater than the corresponding values at HY-2 and HY-1, respectively. Details of the relevant discussion are presented in Section 5.3. The percentages in layers deeper than 2000 m at HY-3, HY-6, HY-9, and HY-11 were higher than the corresponding values for the other stations.

The $^{239+240}\text{Pu}$ and ^{238}Pu inventories and the $^{238}\text{Pu}/^{239+240}\text{Pu}$ inventory ratio are plotted against the longitude in Fig. 6. Only a few $^{239+240}\text{Pu}$ inventories for the mid-latitude region in the South Pacific have been reported previously. The inventories reported by Hirose et al. (2007) were 8 Bq/m² at 15° S 148° W, 12 Bq/m² at 21.75° S 138.9° W, and 8 Bq/m² at 32.5° S 177.7° E. These values are comparable with the $^{239+240}\text{Pu}$ inventories in the South Pacific that we measured. Furthermore, the inventories in the regions HY-1 to HY-3 and HY-11 to HY-18, which are close to one another in latitude, were also comparable. On the other hand, the inventory of ^{238}Pu and its ratio to $^{239+240}\text{Pu}$ tended to be larger in the west than in the east, except in the case of HY-9, HY-11, and HY-12; this is probably due to inflow from the Indian Ocean of ^{238}Pu from SNAP-9a.

The $^{239+240}\text{Pu}$ inventory in each 1000 m of water column is plotted against the corresponding latitude in Fig. 7. For comparison, the inventories from the surface to the bottom in the region between 170° E and 170° W (Bowen et al., 1980) and the inventories from the surface to 2000 m in the region between 140° W and 160° W (Nakano and Povinec, 2003) are also shown in the same figure. The inventories measured by Nakano and Povinec (2003) in the South Pacific

region were around twice those that we found at stations HY-11 to HY-18 in the South East Pacific. If we compare the present results with the $^{239+240}\text{Pu}$ inventories measured by Bowen et al. (1980) and the inventory from the surface to 2500 m in the Arabian Sea, reported by Mulsow et al. (2003), the inventories at the HY stations were closer to those in the Arabian Sea.

The upper layer of the oceanic current moves in a symmetrical manner about the Equator. However, the movement of water no longer follows the surface oceanic current at the depth at which the Pu concentration is maximal. In the Central Pacific, the Pu inventory along a line of longitude showed a distribution that was symmetrical about the Equator. The distribution in the Central Pacific was not reproduced in the inventories for 0–1000 m or 1000–2000 m for the East Pacific. The inventory at HY-6 was typical for the North Pacific, and the inventories at stations HY-9 and HY-11 were higher than were those at stations HY-12 to HY-18. This phenomenon cannot be explained without the presence of a horizontal migration from a Pu-rich region. The Equatorial Under Current is the only current that carries water from west to east at a depth of 100–200 m. However, the reported Pu concentration in the Central Pacific (Livingston et al., 2001) at the depth of the Equatorial Under Current of 100–200 m is too low to explain the increase in the inventory at HY-6.

There is another possible explanation for the high inventory at HY-6. Maximal levels of nutrients was observed at a depth of 700–1000 m, with values of 3.2–3.4 μM for phosphate and 45–46 μM for nitrate at stations HY-1, HY-2, and HY-3. The concentrations of phosphate and nitrate were typical of those for mid-latitudes of the North East Pacific, as reported in the WOCE data (Schlitzer, 2007). However, concentrations of phosphate and nitrate typical of those for mid-latitudes of the North East Pacific were observed at 20° S on the WOCE P18 line (103° E to 110° E) and P19 line (85.5° E–88° E) at a depth of ~1000 m. Maxima of 3.0–3.3 μM for phosphate and 42–47 μM for nitrate at depths of 700–1000 m were observed at HY-6, HY-9, and HY-11, and maxima for phosphate of around 3 μM at HY-12, 2.5 μM at HY-15A, HY-17, and HY-18, and 43

μM at HY-12, 38 μM at HY-15A, and 37 μM at HY-17 and HY-18 were observed in the present work. Increased concentrations of nutrients were observed in the region west of 100° E on the WOCE P21 line (17° S), but not on the WOCE P06 line (32.5° S). In addition, trends similar to those for phosphate and nitrate were observed in the DO distribution. On the other hand, a minimum salinity of 35.5 near 800 m has been observed in both hemispheres in the region between 15° N and 15° S of the entire Pacific (Tomczak and Godfrey, 2005). The difference in salinity near the Equator is not sufficiently significant to permit information on horizontal migration to be inferred from the salinity distribution. The features of the distributions of Pu, DO, and nutrient seen in the region of HY-1, HY-2, and HY-3 are also observed in the region of HY-6, HY-9, and HY-11. These nutrient levels and DO support the theory that Pu migrates from the Northern Hemisphere to the South Hemisphere across the Equator in the East Tropical Pacific. Horizontal migration across the Equator might explain the high Pu inventories at stations HY-6, HY-9, and HY-11.

5.2. Comparison of Pu concentrations in seawater with results of previous work

There are several earlier sets of data pertaining to locations HY-2 and HY-18 that can be examined in conjunction with the results of the present study. Residence times of Pu in surface water have been reported to be 5 yr at HY-2 and 9 yr at HY-18 (Hirose and Aoyama, 2003). The maximum subsurface activity of $^{239+240}\text{Pu}$ at the HY-2 station was observed at 600 m. In 1973, the corresponding maximum at the same location was observed at 500 m (Nakano and Povinec, 2003). Therefore, the Pu maximum had shifted downward by 100 m during 30 yr, and the average velocity of the shift was calculated to be 3.3 m/yr, assuming a constant velocity. At station HY-18, the subsurface Pu maximum was observed at a depth of 700 m in 1996, whereas it was observed at 800 m in 2003. The depth of the maximum Pu level had therefore shifted downward by 100 m in 7 yr, and the sinking velocity was therefore estimated to be 14 m/yr. Furthermore, the subsurface

maximum in the activity of $^{239+240}\text{Pu}$ near Bikini Atoll in the Central Pacific was observed at 850 m in 1997 and at 450 m in 1973. The sinking velocity of the subsurface maximum in Pu was therefore estimated to be approximately 17 m/yr. The velocity at station HY-2 is therefore markedly slower than that near Bikini Atoll. In addition, it has been reported that the maximum in Pu activity has been moving to a deeper layer at an almost constant velocity (Livingston et al., 2001).

5.3. Comparisons with dissolved oxygen, potential temperature, and potential density

Pu atoms can adopt one of four possible oxidation states: III, IV, V, or VI. It is possible that DO could control the oxidation state of Pu. Tri- and tetravalent Pu occur as Pu^{3+} and Pu^{4+} ions, respectively, whereas penta- and hexavalent Pu occur as PuO_2^+ and PuO_2^{2+} , respectively, in aqueous solution. The residence time of tri- and tetravalent Pu in seawater is considered to be ~30 yr, assuming that these show the same behavior as the corresponding thorium species. On the other hand, the residence time of penta- and hexavalent Pu is of the order of 5×10^5 yr, based on the behavior of uranium in the form of the UO_2^{2-} ion in seawater. As can be seen in Table 2, there was a high DO content in the surface waters, an oxygen-deficient layer at 250–1000 m, and an increase in DO near the ocean bottom at stations HY-1 to HY-11. On the other hand, a DO-rich layer caused by AAIW was observed at a depth of ~700 m at stations HY-12 to HY-18. As described in Section 4, subsurface Pu maxima were observed at 500 m for HY-11, 800 m for HY-17 and HY-18, and 600 m for the other stations. The Pu was therefore enriched in the DO-deficient layer at HY-1 to HY-11, whereas it was enriched in the DO-rich layer at HY-12 to HY-18. No clear correlation between the sinking behavior of Pu and DO was therefore observed.

The temperature of seawater is a useful tool in studying vertical diffusion in surface waters. Contour displays of the potential temperature from the surface to a depth of 500 m are shown in Fig. 8, together with the corresponding contour lines of $^{239+240}\text{Pu}$ activity. In Figs. 8(b) and 8(c), the temperature data for the stations HY-4 (4° 00' N 95° 00' W), HY-5 (2° 00' N 95° 30' W), HY-7 (2°

00' S 95° 00' W), HY-8 (4° 00' S 95° 00' W), HY-13 (22° 15' S 108° 00' W), HY-14A (23° 30' S 112° 00' W), HY-14B (24° 15' S 114° 00' W), HY-15B (25° 30' S 118° 00' W), and HY-16 (26° 00' S 120° 00' W) were used to construct the contours. The temperatures at depths of 0–100 m at HY-6, HY-11, and HY-17 are lower by 2–3 °C than are those at neighboring stations of similar longitude. The $^{239+240}\text{Pu}$ concentrations at HY-6, HY-11, and HY-17 at depths of 0–100 m are higher than are those at the neighboring stations. Whereas a layer with a temperature of above 20 °C diffuses down to 200 m at HY-1, to 100 m at HY-2, and to 50 m at HY-3, a layer of $^{239+240}\text{Pu}$ concentration below 2 mBq/m³ is seen at a depth of less than 200 m at HY-1 and 50 m at HY-2 and HY-3. The distribution of the $^{239+240}\text{Pu}$ concentration correlates well with the isothermal line at depths shallower than 400 m. The vertical diffusion may therefore control the Pu distribution at depths from the surface to ~200 m. In particular, upwelling of seawater from 50 m at HY-6 and from 100–200 at HY-11 and HY-17 m may explain the higher Pu concentrations found in the surface waters.

Figure 9 shows the correlation between the $^{239+240}\text{Pu}$ concentration and the potential density sigma- θ . Surprisingly, maxima of $^{239+240}\text{Pu}$ are observed at the depth where sigma- $\theta \approx 27.0$ at all HY stations, although the boundary of the water mass structure does not coincide with depth of the $^{239+240}\text{Pu}$ maximum. The distribution of sigma- θ is markedly dependent on the water mass structure, because each water mass has its own salinity and temperature. It has been reported that more than 99% of Pu at a depth of 250 m is in a non-particle-reactive state (Dai et al., 2001). Pu at depths below 250 m is also considered to be in the same form as that at 250 m. Vertical migration of non-particle-reactive elements such as Pu at depths of 600–800 m is correlated with the density of the seawater.

5.4. Pu activity in sediment

As can be seen in Fig. 4, the vertical profiles of the sediment cores show patterns that differed from one another. For the cores taken at HY-3, a subsurface $^{239+240}\text{Pu}$ maximum was

observed, whereas a marked increase at depths below 7 cm was observed in HY-6. A distribution similar to that which we found has been observed in the Japan Sea (Zheng and Yamada, 2005). These profiles are, primarily, the result of mixing of sediment particles by bioturbation, a process also described as biodiffusional particle mixing (Cochran, 1985), whereas no similar $^{239+240}\text{Pu}$ maximum was found at HY-1, HY-2, or HY-9.

Figure 10 shows the $^{239+240}\text{Pu}$ inventories in sediment in relation to the latitude, together with reported data for the open Pacific (Nagaya and Nakamura, 1987; Hong et al., 1999; Pettersson et al., 1999; Livingston et al., 2001; Moon et al., 2003; Lee et al., 2003; Lee et al., 2005; Zheng and Yamada, 2006; Dong et al., 2010). It is well known that the deposition of anthropogenic radionuclides from all fallout is correlated with the latitude; in other words, maximal deposition is observed in the mid-latitude belt, and minimal deposition is observed in the polar and equatorial regions (Hardy et al., 1973; Baskaran et al., 1996). The peak in $^{239+240}\text{Pu}$ at 10–20° N that can be seen in Fig. 10 is the result of local fallout from the Marshall Islands. The inventories decrease on going from the Marshall Islands to 30–40° N in the Pacific, where the mid-latitude peak originating from global fallout is expected to occur. Higher $^{239+240}\text{Pu}$ inventories observed between 50° and 55° N are due to intense biological activity and high scavenging east of the Kamchatka Peninsula. The figure therefore clearly shows the effects of nuclear bomb test sites and biological activity.

The activity of ^{238}Pu was also detected in the sediment. As shown in Table 4, $^{238}\text{Pu}/^{239+240}\text{Pu}$ inventory ratios in the sediment were calculated to be 0.035 ± 0.013 for HY-1, 0.032 ± 0.012 for HY-2, 0.026 ± 0.006 for HY-3, 0.041 ± 0.007 for HY-6, and 0.021 ± 0.010 for HY-9, whereas the inventory ratios in the seawater column of 0–1000 m were 0.033 ± 0.005 for HY-1, 0.012 ± 0.001 for HY-2, 0.039 ± 0.003 for HY-6, and 0.050 ± 0.003 for HY-9. The $^{238}\text{Pu}/^{239+240}\text{Pu}$ activity ratios in the sediment column correspond closely to those in the seawater column, within the margin of error. This shows that the Pu in the seawater and that in the sediment have the same origin.

The ratios of the $^{239+240}\text{Pu}$ inventory in the water column to those in the sediment column were calculated to be 12.0 for HY-1, 15.0 for HY-2, 5.5 for HY-3, 3.9 for HY-6, and 13.4 for HY-9. The ratios in 1997 in the Western Pacific, between Japan and Bikini Atoll, have been reported to lie in the range 0.9–3.4 (Moon et al., 2003; Povinec et al., 2003). Furthermore, the corresponding ratios for ^{238}Pu are 11.3 for HY-1, 5.6 for HY-2, 3.7 for HY-6, and 32.2 for HY-9. The trend for the water-column/sediment-column ratios at HY-3 and HY-6 to be lower than those at the other stations, is common between $^{239+240}\text{Pu}$ and ^{238}Pu . The percentages of the inventories of ^{238}Pu and $^{239+240}\text{Pu}$ below 1000 m at stations HY-3, HY-6, and HY-9, as shown in Table 4, are also higher than those at the other stations. In addition, the $^{239+240}\text{Pu}$ concentrations below 1000 m in the regions of HY-3, HY-6, and HY-9 are higher than those at other stations, as seen in Fig. 5. The values for stations HY-3, HY-6, and HY-9 were close to those of the continent, in contrast to the other stations; it is therefore presumed that substances originating from the continent affect these results. Consequently, the seawater and sediment data indicate that scavenging in the East Pacific is more active than that elsewhere.

Conclusion

Depth profiles of ^{238}Pu and $^{239+240}\text{Pu}$ in seawater and sea sediment samples taken from the Tropical East Pacific in 2003 were measured. By comparing the results with nutrient data, horizontal migration from the north to the south across the Equator is invoked to explain the high Pu inventories at stations HY-6, HY-9, and HY-11. Furthermore, $^{239+240}\text{Pu}$ activity was also compared with profiles of DO, potential temperature, and sigma- θ . Although it has been proposed that the sinking behavior of Pu could be affected by changes in its valence state under different redox condition as a result of the presence of DO, no notable difference due to DO was observed. On the other hand, the distribution of Pu at depths of 0–400 m correlated with that of the potential

temperature, and the layer of subsurface Pu maximum was observed at a depth where $\sigma\text{-}\theta \approx 27.0$. Various profiles of Pu were observed in samples of sea sediment. A comparison of the inventory ratios of the water column to that in the sediment column and the inventory in each 1000 m of seawater showed that scavenging of Pu at HY-3, HY-6, and HY-9 is more active than that at other stations.

Acknowledgements

We wish to thank Captain T. Seino and the officers and crew of *R.V. Hakuho-Marui*, and the scientific staff of the KH-03-1 cruise (Hydra expedition) for their assistance with the shipboard sampling.

Reference

- Aarkrog A. Input of anthropogenic radionuclides into the world ocean. *Deep-Sea Res II* 2003; 50: 2597–2606.
- Amakawa H, Sasaki K, Ebihara M. Nd isotopic composition in the central North Pacific. *Geochim Cosmochim Acta* 2009; 73: 4705–4719.
- Aston SR. Evaluation of the chemical forms of plutonium in seawater. *Mar Chem* 1980; 8: 319–325.
- Baskaran M, Asbill S, Santschi P, Brooks J, Champ M, Adkinson D, Colmer MR, Makeyev V. Pu, ^{137}Cs and excess ^{210}Pb in Russian Arctic sediments. *Earth Planet Sci Lett* 1996; 140: 243–257.
- Bowen VT, Noshkin VE, Livingston HD, Volchok HL. Fallout radionuclides in the Pacific Ocean: Vertical and horizontal distributions, largely from GEOSECS station. *Earth Planet Sci Lett* 1980; 49: 411–434.
- Buesseler KO, Sholkovitz ER. The geochemistry of fallout plutonium in the North Atlantic: II. $^{240}\text{Pu}/^{239}\text{Pu}$ ratios and their significance. *Geochim Cosmochim Acta* 1987; 51: 2623–2637.
- Buesseler KO. The isotopic signature of fallout plutonium in the north Pacific. *J Environ Radioact* 1997; 36: 69–83.
- Cochran JK. Particle mixing rates in sediments of the eastern equatorial Pacific: Evidence from ^{210}Pb , $^{239,240}\text{Pu}$ and ^{137}Cs distribution at MANOP sites. *Geochim Cosmochim Acta* 1985; 49: 1195–1210.
- Cooper LW, Kelley JM, Bond LA, Orlandini KA, Grebmeier J M. Sources of the transuranic elements plutonium and neptunium in arctic marine sediments. *Mar Chem* 2000; 69: 253–276.
- Dai MH, Buesseler KO, Kelly JM, Andrews JE, Pike S, Wacker JF. Size-fractionated plutonium isotopes in a coastal environment. *J Environ Radioact* 2001; 53: 9–25.

- Doney SC. Bomb tritium in the deep north Atlantic. *Oceanogr* 1992; 5: 169–170.
- Dong W, Zheng J, Guo Q, Yamada M, Pan S. Characterization of plutonium in deep-sea sediments of the Sulu and South China Seas. *J Environ Radioact* 2010; 101: 622–629.
- Fiedler PC. The annual cycle and biological effects of the Costa Rica Dome. *Deep-Sea Res I* 2002; 49: 321–338.
- Hardy EP, Krey PW, Volchok HL. Global inventory and distribution of fallout plutonium. *Nature* 1973; 241: 444–445.
- Harley JH. Plutonium in the environment –A review. *J Radiat Res* 1980; 21: 83–104.
- Hirose K, Aoyama M. Analysis of ^{137}Cs and $^{239,240}\text{Pu}$ concentrations in surface waters of the Pacific Ocean. *Deep-Sea Res II* 2003; 50: 2675–2700.
- Hirose K, Aoyama M, Kim CS. Plutonium in seawater of the Pacific Ocean. *J Radioanal Nucl Chem* 2007; 274: 635–638.
- Hong GH, Lee SH, Kim SH, Chung CS, Baskaran M. Sedimentary fluxes of ^{90}Sr , ^{137}Cs , $^{239,240}\text{Pu}$ and ^{210}Pb in the East Sea (Sea of Japan). *Sci Tot Environ* 1999; 237/238: 225–240.
- Kawabe M, Taira K. Water masses and properties at 165 °E in the western Pacific. *J Geophys Res* 1998; 103: 12941–12958.
- Kelley JM, Bond LA, Beasley TM. Global distribution of Pu isotopes and ^{237}Np . *Sci Tot Environ* 1999; 237/238: 483–500.
- Kershaw PJ, Denoon DC, Woodhead DS. Observations on the redistribution of plutonium and americium in the Irish Sea sediments, 1978 to 1996: Concentrations and inventories. *J Environ Radioact* 1999; 44: 191–221.
- Kinoshita N, Sato Y, Yamagata T, Nagai H, Yokoyama A, Nakanishi T. Incorporation rate measurements of ^{10}Be , ^{230}Th , ^{231}Pa , and $^{239,240}\text{Pu}$ radionuclides in manganese crust in the Pacific Ocean: A search for extraterrestrial material. *J Oceanogr* 2007; 63: 813–820.
- Lagerloef G, Lukas R, Bonjean F, Gunn JT, Mitchum GT, Bourassa M, Busalacchi AJ. El Niño

- Tropical Pacific Ocean surface current and temperature evolution in 2002 and outlook for early 2003. *Geophys Res Lett* 2003; 30: 1514.
- Lee SH, Gastaud J, Povinec PP, Hong GH, Kim SH, Chung CS, Lee KW, Pettersson HBL. Distribution of plutonium and americium in the marginal seas of the Northwest Pacific Ocean. *Deep-Sea Res II* 2003; 50: 2727–2750.
- Lee SH, Povinec PP, Wyse E, Pham MK, Hong GH, Chung CS, Kim SH, Lee HJ. Distribution and inventories of ^{90}Sr , ^{137}Cs , ^{241}Am and Pu isotopes in sediments of the northwest Pacific Ocean. *Mar Geol* 2005; 216: 249–263.
- Livingston HD, Povinec PP, Ito T, Togawa O. The behaviour of plutonium in the Pacific Ocean. In Kudo A, editor. *Plutonium in the Environment*. Elsevier Science, Amsterdam; 2001. p. 267–292.
- Moon DS, Hong GH, Kim YI, Baskaran M, Chung CS, Kim SH, Lee HJ, Lee SH, Povinec PP. Accumulation of anthropogenic and natural radionuclides in bottom sediments of the Northwest Pacific Ocean. *Deep-Sea Res II* 2003; 50: 2649–2673.
- Mulsow S, Povinec PP, Somayajulu BLK, Oregioni B, Liang L, Kwong LLW, Gastaud J, Top Z, Morgenstern U. Temporal (^3H) and spatial variation of ^{90}Sr , $^{239,240}\text{Pu}$ and ^{241}Am in the Arabian Sea: GEOSECS Stations revisited. *Deep-Sea Res II* 2003; 50: 2761–2775.
- Nagaya Y, Nakamura K. Artificial radionuclides in the Western Northwest Pacific (II): ^{137}Cs and $^{239,240}\text{Pu}$ inventories in water and sediment column observed from 1980 to 1986. *J Oceanogr Soc Jap* 1987; 43: 345–355.
- Nakano M, Povinec PP. Modeling the distribution of plutonium in the Pacific Ocean. *J Environ Radioact* 2003; 69: 85–106.
- Paul M, Valenta A, Ahmad I, Berkovits D, Bordeanu C, Ghelberg S, Hashimoto Y, Hershkowitz A, Jiang S, Nakanishi T, Sakamoto K. Experimental limit to interstellar ^{244}Pu abundance. *Astrophys J* 2001; 558: L133–L135.

- Periáñez R. Modeling the distribution of radionuclides in deep ocean water columns. Application to ^3H , ^{137}Cs and $^{239,240}\text{Pu}$. *J Environ Radioact* 1998; 38: 173–194.
- Perkins RW, Thomas CW. Worldwide fallout. In Hanson WC, editor. *Transuranic Elements in the Environment*. DOE/TIC-22800, National Technical Information Center, Springfield, VA; 1980. p. 53–82.
- Pettersson HBL, Amano H, Berezhnov VI, Chaykovskaya E, Chumichev VB, Chung CS, Gastaud J, Hirose K, Hong GH, Kim CK, Lee SH, Morimoto T, Nikitin A, Oda K, Povinec PP, Suzuki E, Tkalin A, Togawa O, Veletova NK, Volkov Y, Yoshida K. Anthropogenic radionuclides in sediments in the NW Pacific Ocean and its marginal seas: results of the 1994–1995 Japanese-Korean-Russian expeditions. *Sci Tot Environ* 1999; 237/238: 213–224.
- Povinec PP, Livingston HD, Shima S, Aoyama M, Gastaud J, Goroncy I, Hirose K, Huynh-Ngoc L, Ikeuchi Y, Ito T, La Rosa J, Liong Wee Kwong L, Lee SH, Moriya H, Mulsow S, Oregioni B, Pettersson H, Togawa O. IAEA'97 expedition to the NW Pacific Ocean—results of oceanographic and radionuclide investigations of the water column. *Deep-Sea Res II* 2003; 50: 2607–2637.
- Sano Y, Takahata N, Gamo T. Helium isotopes in south Pacific deep seawater. *Geochem J* 1995; 29: 377–384.
- Schlitzer R. eWOCE - Electronic Atlas of WOCE Data. Alfred Wegener Institute for Polar and Marine Research, Bremerhaven, Germany. 2007; <http://www.ewoce.org/>.
- Tomczak M, Godfrey JS. *Regional Oceanography: An Introduction*. Elsevier Science; 2005. p. 148.
- Tosaki Y, Tase N, Massmann G, Nagashima Y, Seki R, Takahashi T, Sasa K, Sueki K, Matsuhiro T, Miura T, Bessho K, Matsumura H, He M. Application of ^{36}Cl as a dating tool for modern groundwater. *Nucl Instr Meth B* 2007; 259: 479–485.
- Tourigny E, Jones CG. An analysis of regional climate model performance over the tropical Americas. Part I: Simulating seasonal variability of precipitation associated with ENSO

forcing. *Tellus A* 2009; 61: 323–342.

UNSCEAR. Sources and effects of ionizing radiation. United Nations Scientific Committee on the Effects of Atomic Radiation, United Nations, New York; 2000.

Wallner C, Faestermann T, Gerstmann U, Hillebrandt W, Knie K, Korschinek G, Lierse C, Pomar C, Rugel G. Development of a very sensitive AMS method for the detection of supernova-produced longliving actinide nuclei in terrestrial archives. *Nucl Instr Meth B* 2000; 172: 333–337.

Yamada M, Wang ZL. ^{137}Cs in the western South Pacific Ocean. *Sci Tot Env* 2007; 382: 342–350.

You Y. The pathway and circulation of North Pacific Intermediate Water. *Geophys. Res Lett* 2003; 30: 2201, doi:10.1029/2003GL018561.

Zheng J, Yamada M. Vertical distribution of $^{239+240}\text{Pu}$ activities and $^{240}\text{Pu}/^{238}\text{Pu}$ atom ratios in sediment cores: Implications for the sources of Pu in the Japan Sea. *Sci Tot Env* 2005; 340: 199–211.

Zheng J, Yamada M. Plutonium isotopes in settling particles: Transport and scavenging of Pu in the Western Northwest Pacific. *Environ Sci Technol* 2006; 40: 4103–4108.

Figure captions

Fig. 1

The locations of sampling stations HY-1 to HY 18 where Pu isotopes were measured.

Fig. 2

Potential temperature vs. salinity (θ - S) diagrams for each HY station.

Fig. 3

Vertical profiles of ^{238}Pu and $^{239+240}\text{Pu}$ activities in seawater. The ^{238}Pu activities are indicated by open squares and the $^{239+240}\text{Pu}$ activities are indicated by closed circles.

Fig. 4

Vertical profiles of ^{238}Pu and $^{239+240}\text{Pu}$ activities in sea sediment. The ^{238}Pu activities are indicated by open squares and $^{239+240}\text{Pu}$ activities are indicated by closed circles.

Fig. 5

Geographical distribution of $^{239+240}\text{Pu}$ along the cruising course. (a): HY-1 to HY-3, (b) HY-3 to HY-9, (c) HY-11 to HY-18.

Fig. 6

Longitudinal distribution of $^{239+240}\text{Pu}$ inventory (a), ^{238}Pu inventory (b), and $^{238}\text{Pu}/^{239+240}\text{Pu}$ inventory ratio (c) in seawater. The data for the North, Equatorial, and South Pacific are plotted with red circles, green triangle, and blue squares, respectively. The $^{238}\text{Pu}/^{239+240}\text{Pu}$ inventory ratio in sediment was used for estimation at station HY-3 because of a lack of ^{238}Pu data for depths of

0–1000 m.

Fig. 7

Latitudinal distributions of $^{239+240}\text{Pu}$ inventory. $^{239+240}\text{Pu}$ inventories at 0–1000 m (red circles), 1000–2000 m (green triangles), 2000–3000 m (blue squares) are plotted. In addition, the inventories for the water column for the region 170° E to 170° W (Bowen et al., 1980; the inventory is multiplied by 1/5), for the region 140° W to 160° W (Nakano and Povinec, 2003), and for the region 50° W to 70° W (Mulsow et al., 2003) are also drawn.

Fig. 8

Geographical distribution of potential temperature along the cruising course. The contour lines show the $^{239+240}\text{Pu}$ activity (mBq/m^3). (a): HY-1 to HY-3, (b): HY-3 to HY-9, (c): HY-11 to HY-18.

Fig. 9

Vertical profiles of $^{239+240}\text{Pu}$ concentration plotted against the potential density ($\sigma\text{-}\theta$).

Fig. 10

Latitudinal distribution of $^{239+240}\text{Pu}$ inventory in sediment. Results from this work are plotted as closed circles and data from previous reports are plotted as open squares.

Table captions

Table 1

Location of the stations, the water depths, and the sampling dates.

Table 2

Depth profile data of the potential temperature (P. Temp), salinity, potential density (σ_θ), dissolved oxygen (DO), and radioactivities of ^{238}Pu and $^{239+240}\text{Pu}$ in seawater. Because ^{238}Pu tracer was used in some of the samples from HY-3 to check the yield of the chemical protocol, ^{238}Pu was not determined in some of HY-3 samples. N.D. = “Not Detected” (below the detection limit).

Table 3

Depth profiles of radioactivity of ^{238}Pu and $^{239+240}\text{Pu}$ in sea sediment samples.

Table 4

Inventory, percentage of $^{239+240}\text{Pu}$, and $^{238}\text{Pu}/^{239+240}\text{Pu}$ activity ratio at each depth in the water column and in sediment.

Station	Location	Water depth	Sampling date
HY-1	20°00' N 140°00' W	5309 m	June 28, 2003
HY-2	16° 31' N 123° 00' W	4208 m	July 2, 2003
HY-3	8° 02' N 95° 27' W	3635 m	July 7, 2003
HY-6	0° 01' N 95° 27' W	3219 m	July 10, 2003
HY-9	7° 59' S 95° 01' W	3882 m	July 14, 2003
HY-11	15° 08' S 85° 50' W	4680 m	July 26, 2003
HY-12	20° 00' S 101° 00' W	4114 m	July 30, 2003
HY-15A	25° 00' S 116° 00' W	2867 m	Aug. 2, 2003
HY-17	28° 30' S 127° 47' W	4037 m	Aug. 5, 2003
HY-18	26° 00' S 140° 00' W	4411 m	Aug. 8, 2003

Table 1

HY-1 (20°00'N, 140°00'W)							HY-2 (16°31'N, 123°00'W)						
Depth	P.Temp	Salinity	σ_θ	DO	^{238}Pu	$^{239+240}\text{Pu}$	Depth	P.Temp	Salinity	σ_θ	DO	^{238}Pu	$^{239+240}\text{Pu}$
(m)	(°C)		(kg/m^3)	(L/m^3)	(mBq/m^3)	(mBq/m^3)	(m)	(°C)		(kg/m^3)	(L/m^3)	(mBq/m^3)	(mBq/m^3)
6	24.152	34.713	23.379	4.51	N.D.	1.0 ± 0.2	6	25.150	34.449	22.879	4.38	0.3 ± 0.2	0.8 ± 0.2
99	22.217	35.096	24.230	4.68	N.D.	0.8 ± 0.2	101	20.428	34.645	24.378	4.82	0.3 ± 0.2	7.6 ± 0.6
256	14.049	34.284	25.623	3.28	N.D.	2.4 ± 0.5	247	11.327	34.686	26.471	0.09	0.6 ± 0.2	3.7 ± 0.4
395	9.076	34.256	26.602	1.27	N.D.	18.0 ± 1.2	397	9.173	34.578	26.760	0.11	1.3 ± 0.3	25.9 ± 2.1
600	6.732	34.435	27.010	0.32	N.D.	31.4 ± 3.0	594	6.841	34.595	27.043	0.23	0.4 ± 0.2	52.6 ± 3.6
795	5.226	34.461	27.222	0.46	0.6 ± 0.1	23.0 ± 2.5	796	5.597	34.517	27.221	0.18	0.6 ± 0.3	29.8 ± 2.3
1000	4.333	34.489	27.351	0.69	0.7 ± 0.2	17.0 ± 0.8	989	4.560	34.528	27.351	0.38	N.D.	25.2 ± 2.4
1500	2.883	34.577	27.558	0.94	N.D.	5.2 ± 0.8	1490	2.970	34.589	27.560	1.16	N.D.	9.9 ± 1.8
2000	2.008	34.623	27.669	1.88	N.D.	2.8 ± 0.3	1989	2.104	34.632	27.669	1.46	N.D.	4.9 ± 1.3
2485	1.568	34.652	27.726	2.31	N.D.	2.5 ± 0.3	2486	1.657	34.656	27.723	1.78	N.D.	6.2 ± 0.7
2983	1.362	34.671	27.756	2.61	N.D.	2.3 ± 0.3	2984	1.413	34.672	27.753	2.26	N.D.	5.7 ± 0.5
3481	1.233	34.680	27.773	2.85	N.D.	2.5 ± 0.3	3487	1.280	34.680	27.769	2.57	N.D.	5.0 ± 0.6
4011	1.142	34.687	27.785	3.09	1.6 ± 0.5	4.2 ± 0.3	3983	1.220	34.684	27.776	2.77	N.D.	6.0 ± 0.6
4485	1.059	34.694	27.795	3.34	N.D.	4.6 ± 0.2	4154	1.194	34.686	27.776	2.89	0.5 ± 0.2	14.7 ± 1.0
4976	1.009	34.697	27.801	3.49	N.D.	7.1 ± 0.3	4208	1.194	34.686	27.780	2.97	N.D.	19.3 ± 1.8
5265	0.999	34.698	27.801	3.50	0.3 ± 0.1	9.8 ± 0.4							
5309	0.999	34.698	27.803	3.50	0.7 ± 0.3	9.8 ± 0.7							

HY-3 (8°02'N, 95°27'W)							HY-6 (0°02'N, 95°27'W)						
Depth	P.Temp	Salinity	σ_θ	DO	^{238}Pu	$^{239+240}\text{Pu}$	Depth	P.Temp	Salinity	σ_θ	DO	^{238}Pu	$^{239+240}\text{Pu}$
(m)	(°C)		(kg/m^3)	(L/m^3)	(mBq/m^3)	(mBq/m^3)	(m)	(°C)		(kg/m^3)	(L/m^3)	(mBq/m^3)	(mBq/m^3)
6	28.745	33.779	21.241	4.17	-	0.6 ± 0.2	6	21.397	34.971	24.374	4.03	0.2 ± 0.1	3.1 ± 0.3
108	13.834	34.914	26.155	0.31	-	11.0 ± 1.3	95	15.653	34.983	25.813	2.49	0.5 ± 0.2	9.0 ± 0.6
247	11.115	34.755	26.564	0.24	-	15.2 ± 1.9	248	13.012	34.926	26.333	1.62	0.7 ± 0.2	12.2 ± 0.8
394	9.585	34.684	26.775	0.09	-	22.3 ± 1.8	404	10.139	34.746	26.729	0.20	0.7 ± 0.1	18.7 ± 0.9
601	6.948	34.582	27.096	0.10	-	35.1 ± 3.2	592	7.752	34.622	27.014	0.62	1.3 ± 0.3	31.6 ± 2.2
794	5.507	34.571	27.275	0.37	0.6 ± 0.1	26.1 ± 1.0	792	5.963	34.562	27.211	1.20	0.4 ± 0.2	29.9 ± 2.3
995	4.545	34.572	27.388	0.85	0.4 ± 0.1	17.3 ± 0.8	989	4.482	34.558	27.383	1.61	0.8 ± 0.2	18.3 ± 1.4
1489	3.155	34.608	27.558	1.32	N.D.	10.5 ± 0.9	1488	3.112	34.602	27.557	1.78	0.6 ± 0.2	11.7 ± 1.2
1990	2.253	34.640	27.662	1.62	N.D.	7.2 ± 0.7	1978	2.156	34.644	27.674	2.02	N.D.	9.3 ± 0.8
2486	1.699	34.667	27.728	1.93	0.2 ± 0.1	6.1 ± 0.6	2479	1.709	34.664	27.725	2.19	0.5 ± 0.1	11.2 ± 0.7
2988	1.600	34.672	27.740	2.30	0.4 ± 0.1	14.4 ± 1.1	2985	1.524	34.677	27.750	2.56	0.9 ± 0.2	11.7 ± 0.6
3484	1.588	34.673	27.741	2.47	N.D.	11.6 ± 0.8	3162	1.515	34.677	27.750	2.77	0.5 ± 0.2	16.7 ± 1.2
3585	1.586	34.674	27.741	2.51	N.D.	18.4 ± 1.4	3214	1.515	34.677	27.750	2.78	0.6 ± 0.2	16.5 ± 1.3
3635	1.586	34.674	27.742	2.51	0.3 ± 0.2	21.4 ± 1.1							

HY-9 (07°59'S, 95°01'W)							HY-11 (15°08'S, 85°50'W)						
Depth	P.Temp	Salinity	σ_θ	DO	^{238}Pu	$^{239+240}\text{Pu}$	Depth	P.Temp	Salinity	σ_θ	DO	^{238}Pu	$^{239+240}\text{Pu}$
(m)	(°C)		(kg/m^3)	(L/m^3)	(mBq/m^3)	(mBq/m^3)	(m)	(°C)		(kg/m^3)	(L/m^3)	(mBq/m^3)	(mBq/m^3)
6	23.952	35.518	24.048	4.43	N.D.	0.9 ± 0.2	6	19.689	35.573	25.281	4.840	N.D.	0.8 ± 0.2
108	15.903	35.083	25.833	0.75	0.2 ± 0.1	2.6 ± 0.3	105	19.575	35.555	25.297	4.770	N.D.	0.8 ± 0.2
250	11.545	34.848	26.557	0.26	3.0 ± 0.5	13.2 ± 1.2	247	11.705	34.810	26.497	0.090	0.5 ± 0.1	5.3 ± 0.4
403	9.575	34.721	26.806	0.18	0.4 ± 0.2	15.8 ± 1.9	395	9.076	34.662	26.841	0.230	1.5 ± 0.2	11.8 ± 0.7
595	6.864	34.576	27.103	0.19	0.5 ± 0.2	17.7 ± 1.4	593	6.743	34.539	27.091	0.520	0.5 ± 0.1	11.2 ± 0.7
793	5.202	34.540	27.287	1.01	1.1 ± 0.3	16.2 ± 1.5	792	5.193	34.510	27.264	0.860	0.3 ± 0.2	9.2 ± 0.6
996	4.336	34.547	27.390	1.57	0.2 ± 0.1	11.3 ± 1.0	1000	4.329	34.533	27.380	1.210	0.3 ± 0.1	8.4 ± 0.7
1491	2.858	34.601	27.580	2.06	0.3 ± 0.2	8.5 ± 0.9	1495	2.864	34.594	27.573	1.870	N.D.	5.9 ± 0.5
1993	2.171	34.640	27.670	2.08	0.2 ± 0.1	7.0 ± 0.5	1991	2.085	34.642	27.678	2.410	0.3 ± 0.1	5.1 ± 0.3
2486	1.750	34.666	27.723	2.27	0.4 ± 0.1	8.3 ± 0.5	2487	1.696	34.668	27.729	2.800	N.D.	3.3 ± 0.3
2989	1.563	34.680	27.749	2.55	0.6 ± 0.1	8.7 ± 0.5	2983	1.578	34.677	27.746	2.900	N.D.	5.4 ± 0.5
3485	1.521	34.684	27.755	2.97	0.3 ± 0.1	9.6 ± 0.6	3481	1.519	34.683	27.755	3.020	N.D.	2.4 ± 0.3
3831	1.517	34.685	27.755	2.95	0.6 ± 0.1	13.3 ± 0.5	3978	1.442	34.689	27.764	3.170	N.D.	3.7 ± 0.3
3882	1.517	34.685	27.755	2.92	0.7 ± 0.1	14.2 ± 0.5	4622	1.421	34.690	27.767	3.180	0.2 ± 0.1	6.4 ± 0.4
							4680	1.419	34.691	27.768	3.180	N.D.	6.2 ± 0.6

Table 2

HY-12 (20°00'S, 101°00'W)							HY-15A (25°00'S, 116°00'W)						
Depth	P.Temp	Salinity	σ_θ	DO	^{238}Pu	$^{239+240}\text{Pu}$	Depth	P.Temp	Salinity	σ_θ	DO	^{238}Pu	$^{239+240}\text{Pu}$
(m)	(°C)		(kg/m^3)	(L/m^3)	(mBq/m^3)	(mBq/m^3)	(m)	(°C)		(kg/m^3)	(L/m^3)	(mBq/m^3)	(mBq/m^3)
6	22.045	36.004	24.968	4.69	N.D.	0.2 ± 0.1	6	22.425	36.222	25.027	4.61	N.D.	0.7 ± 0.1
101	22.048	36.019	24.979	4.70	0.2 ± 0.1	0.4 ± 0.1	101	21.847	36.085	25.086	4.62	0.2 ± 0.1	0.7 ± 0.2
258	13.830	34.631	25.938	4.02	0.2 ± 0.1	0.7 ± 0.2	249	15.989	35.009	25.757	4.44	N.D.	1.0 ± 0.1
398	9.081	34.524	26.733	1.24	0.7 ± 0.2	8.7 ± 0.6	404	9.362	34.405	26.594	3.49	0.3 ± 0.1	2.7 ± 0.2
595	6.246	34.425	27.067	2.19	0.9 ± 0.2	10.1 ± 0.6	598	5.926	34.300	27.009	4.77	0.7 ± 0.2	6.6 ± 0.4
801	5.179	34.461	27.227	1.67	1.3 ± 0.3	6.6 ± 0.6	797	4.797	34.302	27.145	4.13	0.8 ± 0.3	5.1 ± 0.5
990	4.295	34.503	27.360	1.84	0.6 ± 0.3	5.7 ± 0.5	998	4.041	34.417	27.318	3.07	0.7 ± 0.2	5.7 ± 0.7
1500	2.875	34.579	27.560	2.29	0.2 ± 0.1	1.8 ± 0.3	1488	2.451	34.574	27.594	3.19	N.D.	2.1 ± 0.4
1986	2.122	34.631	27.667	2.73	N.D.	1.4 ± 0.2	1993	1.903	34.638	27.689	3.26	N.D.	2.1 ± 0.5
2485	1.723	34.663	27.723	3.20	N.D.	1.1 ± 0.1	2488	1.690	34.660	27.723	3.32	N.D.	1.2 ± 0.3
2978	1.569	34.679	27.747	3.20	N.D.	0.8 ± 0.2	2817	1.651	34.665	27.730	3.32	N.D.	1.4 ± 0.3
3921	1.510	34.686	27.760	3.15	0.2 ± 0.1	3.2 ± 0.1	2867	1.645	34.666	27.730	3.31	0.2 ± 0.1	1.2 ± 0.2
4065	1.491	34.687	27.760	3.14	0.5 ± 0.1	5.4 ± 0.2							
4114	1.490	34.687	27.760	3.12	0.4 ± 0.1	5.9 ± 0.2							

HY-17 (28°30'S, 127°47'W)							HY-18 (26°00'S, 140°00'W)						
Depth	P.Temp	Salinity	σ_θ	DO	^{238}Pu	$^{239+240}\text{Pu}$	Depth	P.Temp	Salinity	σ_θ	DO	^{238}Pu	$^{239+240}\text{Pu}$
(m)	(°C)		(kg/m^3)	(L/m^3)	(mBq/m^3)	(mBq/m^3)	(m)	(°C)		(kg/m^3)	(L/m^3)	(mBq/m^3)	(mBq/m^3)
6	20.228	35.556	25.126	4.82	N.D.	0.7 ± 0.1	6	22.053	35.564	24.631	4.63	N.D.	0.6 ± 0.1
248	15.946	35.125	25.856	4.84	N.D.	1.4 ± 0.8	100	21.678	35.552	24.727	4.68	0.2 ± 0.1	0.6 ± 0.1
398	10.781	34.600	26.503	4.42	0.4 ± 0.1	3.1 ± 0.3	250	17.777	35.461	25.680	4.31	0.2 ± 0.1	0.8 ± 0.1
588	6.690	34.348	26.947	5.20	1.3 ± 0.2	6.5 ± 0.4	399	12.318	34.861	26.420	4.30	0.7 ± 0.2	2.7 ± 0.3
792	5.503	34.287	27.050	5.04	1.1 ± 0.1	8.5 ± 0.4	597	6.892	34.363	26.932	4.90	0.7 ± 0.1	7.2 ± 0.5
988	4.368	34.316	27.203	4.24	1.0 ± 0.2	6.9 ± 0.5	801	5.479	34.299	27.063	4.89	1.2 ± 0.3	9.6 ± 0.6
1492	2.638	34.535	27.546	3.37	0.2 ± 0.1	2.5 ± 0.2	993	4.287	34.338	27.230	4.04	1.1 ± 0.2	8.2 ± 0.5
1990	2.005	34.623	27.669	3.25	N.D.	1.7 ± 0.2	1495	2.563	34.552	27.567	3.34	0.2 ± 0.1	2.4 ± 0.2
2485	1.656	34.657	27.723	3.29	N.D.	0.9 ± 0.1	1989	1.967	34.627	27.676	3.24	N.D.	1.5 ± 0.2
2986	1.441	34.673	27.752	3.45	N.D.	1.6 ± 0.2	2486	1.662	34.656	27.722	3.30	N.D.	1.1 ± 0.1
3461	1.311	34.683	27.769	3.58	N.D.	1.3 ± 0.1	2985	1.464	34.671	27.749	3.42	N.D.	1.7 ± 0.2
3983	1.243	34.688	27.778	3.63	0.2 ± 0.1	1.1 ± 0.2	3487	1.283	34.684	27.772	3.59	0.4 ± 0.2	1.5 ± 0.2
4037	1.239	34.688	27.779	3.63	N.D.	4.9 ± 0.5	3988	1.272	34.687	27.786	3.71	0.2 ± 0.1	1.4 ± 0.2
							4356	1.247	34.694	27.786	3.71	0.3 ± 0.2	3.0 ± 0.2
							4411	1.247	34.694	27.789	3.71	0.5 ± 0.1	3.8 ± 0.4

Table 2 (continued)

Depth (cm)	HY-1 (20°00'N, 140°00'W)		HY-2 (16°31'N, 123°00'W)		HY-3 (8°02'N, 95°27'W)		HY-6 (0°01'N, 95°27'W)		HY-9 (7°59'S, 95°01'W)	
	²³⁸ Pu	²³⁹⁺²⁴⁰ Pu	²³⁸ Pu	²³⁹⁺²⁴⁰ Pu	²³⁸ Pu	²³⁹⁺²⁴⁰ Pu	²³⁸ Pu	²³⁹⁺²⁴⁰ Pu	²³⁸ Pu	²³⁹⁺²⁴⁰ Pu
	(Bq/m ²)	(Bq/m ²)	(Bq/m ²)	(Bq/m ²)	(Bq/m ²)	(Bq/m ²)	(Bq/m ²)	(Bq/m ²)	(Bq/m ²)	(Bq/m ²)
0-1	0.06 ± 0.04	1.67 ± 0.15	0.06 ± 0.02	1.60 ± 0.18	0.06 ± 0.03	1.08 ± 0.15	0.11 ± 0.03	2.19 ± 0.23	N.D.	1.15 ± 0.18
1-2	0.05 ± 0.02	0.11 ± 0.03	0.05 ± 0.04	0.71 ± 0.09	0.05 ± 0.02	1.35 ± 0.19	N.D.	1.48 ± 0.19	N.D.	0.54 ± 0.09
2-3	N.D.	0.15 ± 0.03	N.D.	0.30 ± 0.06	0.06 ± 0.02	1.31 ± 0.16	0.04 ± 0.02	0.99 ± 0.13	0.06 ± 0.03	0.37 ± 0.07
3-4	N.D.	0.14 ± 0.02	N.D.	0.21 ± 0.04	0.04 ± 0.02	1.89 ± 0.22	0.04 ± 0.01	0.98 ± 0.12	N.D.	0.26 ± 0.06
4-5	N.D.	0.37 ± 0.23	N.D.	0.32 ± 0.04	0.03 ± 0.01	1.28 ± 0.15	0.03 ± 0.02	0.73 ± 0.12	N.D.	0.25 ± 0.05
5-6	N.D.	0.24 ± 0.04	N.D.	0.22 ± 0.02	N.D.	1.27 ± 0.17	0.17 ± 0.06	0.42 ± 0.21	N.D.	0.33 ± 0.04
6-7	N.D.	0.34 ± 0.04			N.D.	0.39 ± 0.07	N.D.	1.45 ± 0.48		
7-8	N.D.	0.09 ± 0.03			N.D.	0.29 ± 0.05	0.11 ± 0.04	2.63 ± 0.60		
8-9					N.D.	0.24 ± 0.03	N.D.	0.90 ± 0.08		
9-10							N.D.	0.17 ± 0.02		
10-11							N.D.	0.12 ± 0.02		
11-12							N.D.	0.06 ± 0.01		

Table 3

HY-1 (20°00'N, 140°00'W)					
Depth (m)	²³⁸ Pu (Bq/m ²)	²³⁹⁺²⁴⁰ Pu (Bq/m ²)	²³⁸ Pu (%)	²³⁹⁺²⁴⁰ Pu (%)	²³⁸ Pu/ ²³⁹⁺²⁴⁰ Pu activity ratio
0-1000	0.19 ± 0.02	16.2 ± 0.6	15.5 ± 3.1	43.7 ± 1.8	0.012 ± 0.002
1000-2000	0.18 ± 0.05	7.6 ± 0.4	14.1 ± 4.6	20.4 ± 1.0	0.023 ± 0.007
2000-3000	N.D.	2.5 ± 0.1	0.0 ± 0.0	6.7 ± 0.4	-
3000-bottom	0.87 ± 0.18	10.8 ± 0.2	70.0 ± 18.0	29.1 ± 0.8	0.080 ± 0.017
Sea water	1.24 ± 0.19	37.1 ± 0.7			0.033 ± 0.005
Sediment	0.11 ± 0.04	3.1 ± 0.3			0.035 ± 0.013

HY-2 (16°31'N, 123°00'W)					
Depth (m)	²³⁸ Pu (Bq/m ²)	²³⁹⁺²⁴⁰ Pu (Bq/m ²)	²³⁸ Pu (%)	²³⁹⁺²⁴⁰ Pu (%)	²³⁸ Pu/ ²³⁹⁺²⁴⁰ Pu activity ratio
0-1000	0.56 ± 0.07	24.8 ± 0.7	90.8 ± 15.1	48.5 ± 1.8	0.023 ± 0.003
1000-2000	N.D.	12.5 ± 0.9	0.0 ± 0.0	24.5 ± 1.9	-
2000-3000	N.D.	5.7 ± 0.4	0.0 ± 0.0	11.2 ± 0.9	-
3000-bottom	0.06 ± 0.02	8.1 ± 0.3	9.1 ± 3.1	15.9 ± 0.7	0.007 ± 0.002
Sea water	0.62 ± 0.07	51.1 ± 1.3			0.012 ± 0.001
Sediment	0.11 ± 0.04	3.4 ± 0.2			0.032 ± 0.012

HY-3 (8°02'N, 95°27'W)					
Depth (m)	²³⁸ Pu (Bq/m ²)	²³⁹⁺²⁴⁰ Pu (Bq/m ²)	²³⁸ Pu (%)	²³⁹⁺²⁴⁰ Pu (%)	²³⁸ Pu/ ²³⁹⁺²⁴⁰ Pu activity ratio
0-1000	-	21.4 ± 0.6	-	42.7 ± 1.4	-
1000-2000	0.10 ± 0.02	11.3 ± 0.4	-	22.5 ± 0.9	0.009 ± 0.002
2000-3000	0.20 ± 0.04	8.4 ± 0.4	-	16.8 ± 0.8	0.024 ± 0.005
3000-bottom	0.11 ± 0.03	9.0 ± 0.4	-	17.9 ± 0.8	0.012 ± 0.003
Sea water	-	50.1 ± 0.9			-
Sediment	0.24 ± 0.05	9.1 ± 0.4			0.026 ± 0.006

HY-6 (0°02'N, 95°27'W)					
Depth (m)	²³⁸ Pu (Bq/m ²)	²³⁹⁺²⁴⁰ Pu (Bq/m ²)	²³⁸ Pu (%)	²³⁹⁺²⁴⁰ Pu (%)	²³⁸ Pu/ ²³⁹⁺²⁴⁰ Pu activity ratio
0-1000	0.71 ± 0.06	20.2 ± 0.5	-	42.9 ± 1.1	0.035 ± 0.003
1000-2000	0.50 ± 0.09	12.6 ± 0.6	-	26.8 ± 1.3	0.039 ± 0.007
2000-3000	0.48 ± 0.06	10.9 ± 0.4	-	23.2 ± 0.8	0.044 ± 0.006
3000-bottom	0.15 ± 0.03	3.4 ± 0.1	-	7.2 ± 0.3	0.045 ± 0.008
Sea water	1.84 ± 0.13	47.1 ± 0.8			0.039 ± 0.003
Sediment	0.50 ± 0.08	12.1 ± 0.9			0.041 ± 0.007

HY-9 (07°59'S, 95°01'W)					
Depth (m)	²³⁸ Pu (Bq/m ²)	²³⁹⁺²⁴⁰ Pu (Bq/m ²)	²³⁸ Pu (%)	²³⁹⁺²⁴⁰ Pu (%)	²³⁸ Pu/ ²³⁹⁺²⁴⁰ Pu activity ratio
0-1000	0.87 ± 0.10	12.9 ± 0.4	45.3 ± 5.8	33.1 ± 1.2	0.068 ± 0.008
1000-2000	0.25 ± 0.07	8.8 ± 0.4	12.9 ± 3.5	22.6 ± 1.1	0.028 ± 0.008
2000-3000	0.40 ± 0.05	8.1 ± 0.3	20.7 ± 2.9	20.7 ± 0.8	0.050 ± 0.006
3000-bottom	0.41 ± 0.02	9.2 ± 0.2	21.3 ± 1.9	23.7 ± 0.8	0.045 ± 0.003
Sea water	1.93 ± 0.13	38.9 ± 0.7			0.050 ± 0.003
Sediment	0.06 ± 0.03	2.9 ± 0.2			0.021 ± 0.010

HY-11 (15°08'S, 85°50'W)					
Depth (m)	²³⁸ Pu (Bq/m ²)	²³⁹⁺²⁴⁰ Pu (Bq/m ²)	²³⁸ Pu (%)	²³⁹⁺²⁴⁰ Pu (%)	²³⁸ Pu/ ²³⁹⁺²⁴⁰ Pu activity ratio
0-1000	0.60 ± 0.05	7.9 ± 0.2	72.9 ± 8.7	31.0 ± 0.9	0.076 ± 0.007
1000-2000	0.15 ± 0.04	6.2 ± 0.2	18.1 ± 4.5	24.5 ± 1.0	0.024 ± 0.006
2000-3000	N.D.	4.2 ± 0.2	0.0 ± 0.0	16.7 ± 0.7	-
3000-bottom	0.07 ± 0.03	7.1 ± 0.2	8.6 ± 4.0	27.8 ± 1.0	0.010 ± 0.005
Sea water	0.82 ± 0.07	25.5 ± 0.4			0.032 ± 0.003
Sediment	-	-			-

HY-12 (20°00'S, 101°00'W)					
Depth (m)	²³⁸ Pu (Bq/m ²)	²³⁹⁺²⁴⁰ Pu (Bq/m ²)	²³⁸ Pu (%)	²³⁹⁺²⁴⁰ Pu (%)	²³⁸ Pu/ ²³⁹⁺²⁴⁰ Pu activity ratio
0-1000	0.67 ± 0.06	5.5 ± 0.1	61.3 ± 9.0	45.4 ± 1.7	0.121 ± 0.012
1000-2000	0.25 ± 0.08	2.7 ± 0.2	23.2 ± 8.1	22.3 ± 1.5	0.094 ± 0.032
2000-3000	N.D.	1.1 ± 0.1	0.0 ± 0.0	9.2 ± 0.6	-
3000-bottom	0.17 ± 0.05	2.8 ± 0.1	15.3 ± 4.7	22.9 ± 1.0	0.060 ± 0.018
Sea water	1.09 ± 0.12	12.1 ± 0.3			0.090 ± 0.010
Sediment	-	-			-

HY-15A (25°00'S, 116°00'W)					
Depth (m)	²³⁸ Pu (Bq/m ²)	²³⁹⁺²⁴⁰ Pu (Bq/m ²)	²³⁸ Pu (%)	²³⁹⁺²⁴⁰ Pu (%)	²³⁸ Pu/ ²³⁹⁺²⁴⁰ Pu activity ratio
0-1000	0.44 ± 0.06	3.6 ± 0.1	71.7 ± 12.2	45.9 ± 2.3	0.123 ± 0.016
1000-2000	0.17 ± 0.05	3.0 ± 0.2	27.7 ± 8.5	37.5 ± 3.4	0.058 ± 0.017
2000-3000	N.D.	1.3 ± 0.1	0.0 ± 0.0	16.6 ± 2.0	-
3000-bottom	-	-	-	-	-
Sea water	0.62 ± 0.07	7.9 ± 0.3			0.078 ± 0.010
Sediment	-	-			-

HY-17 (28°30'S, 127°47'W)					
Depth (m)	²³⁸ Pu (Bq/m ²)	²³⁹⁺²⁴⁰ Pu (Bq/m ²)	²³⁸ Pu (%)	²³⁹⁺²⁴⁰ Pu (%)	²³⁸ Pu/ ²³⁹⁺²⁴⁰ Pu activity ratio
0-1000	0.99 ± 0.07	4.6 ± 0.2	94.7 ± 10.0	42.5 ± 1.6	0.218 ± 0.018
1000-2000	N.D.	3.4 ± 0.2	0.0 ± 0.0	32.2 ± 1.5	-
2000-3000	0.05 ± 0.03	1.3 ± 0.1	5.0 ± 2.5	12.0 ± 0.8	0.041 ± 0.021
3000-bottom	0.01 ± 0.00	1.5 ± 0.1	0.5 ± 0.3	13.6 ± 0.8	0.004 ± 0.002
Sea water	1.05 ± 0.08	10.7 ± 0.2			0.098 ± 0.008
Sediment	-	-			-

HY-18 (26°00'S, 140°00'W)					
Depth (m)	²³⁸ Pu (Bq/m ²)	²³⁹⁺²⁴⁰ Pu (Bq/m ²)	²³⁸ Pu (%)	²³⁹⁺²⁴⁰ Pu (%)	²³⁸ Pu/ ²³⁹⁺²⁴⁰ Pu activity ratio
0-1000	0.98 ± 0.08	4.8 ± 0.1	70.3 ± 8.3	39.2 ± 1.2	0.203 ± 0.017
1000-2000	0.05 ± 0.02	3.6 ± 0.1	3.6 ± 1.8	29.5 ± 1.3	0.014 ± 0.007
2000-3000	0.10 ± 0.05	1.3 ± 0.1	7.2 ± 3.7	10.9 ± 0.6	0.075 ± 0.038
3000-bottom	0.26 ± 0.07	2.5 ± 0.1	19.0 ± 5.3	20.5 ± 0.9	0.105 ± 0.028
Sea water	1.39 ± 0.12	12.3 ± 0.2			0.113 ± 0.010
Sediment	-	-			-

Table 4

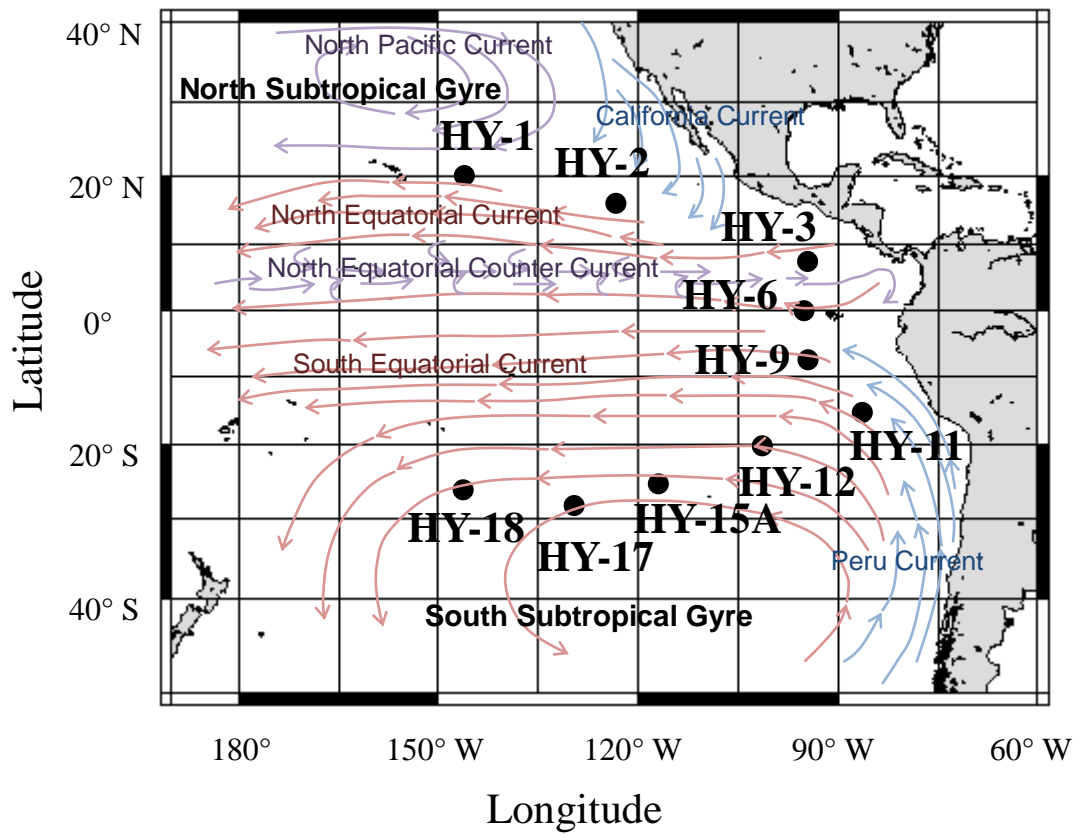


Fig. 1

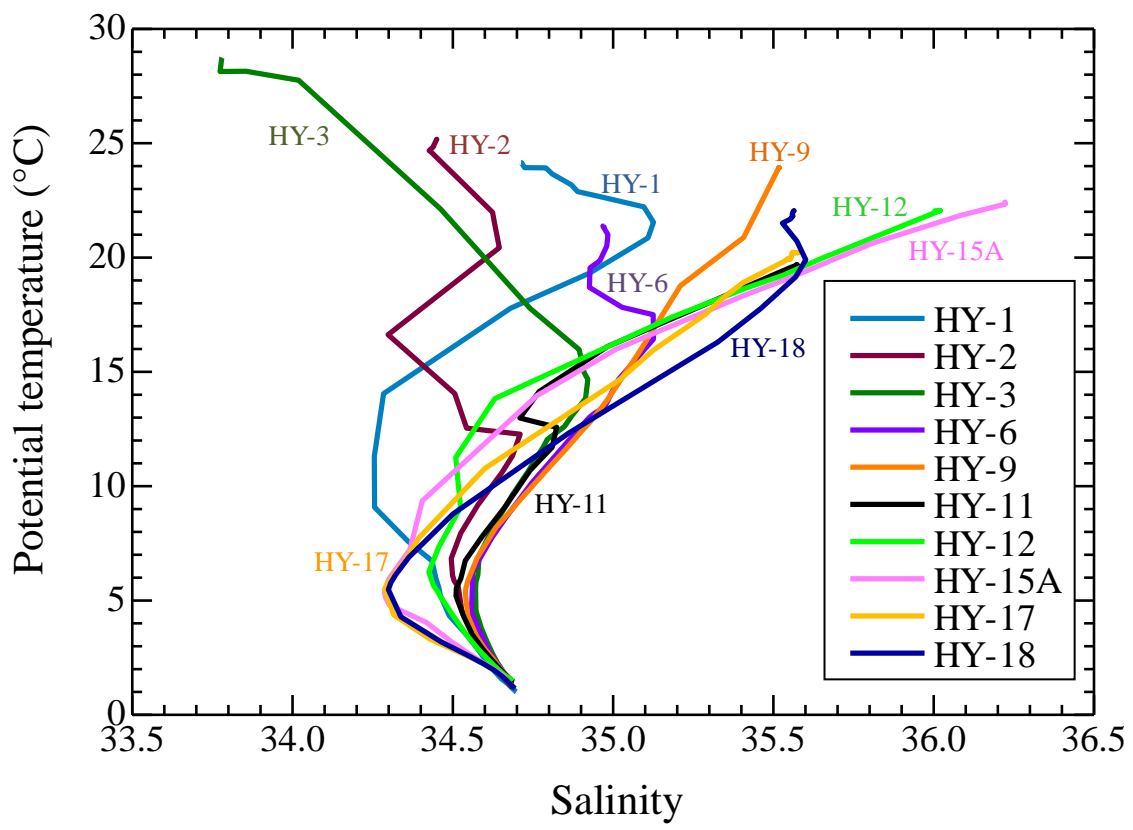


Fig. 2

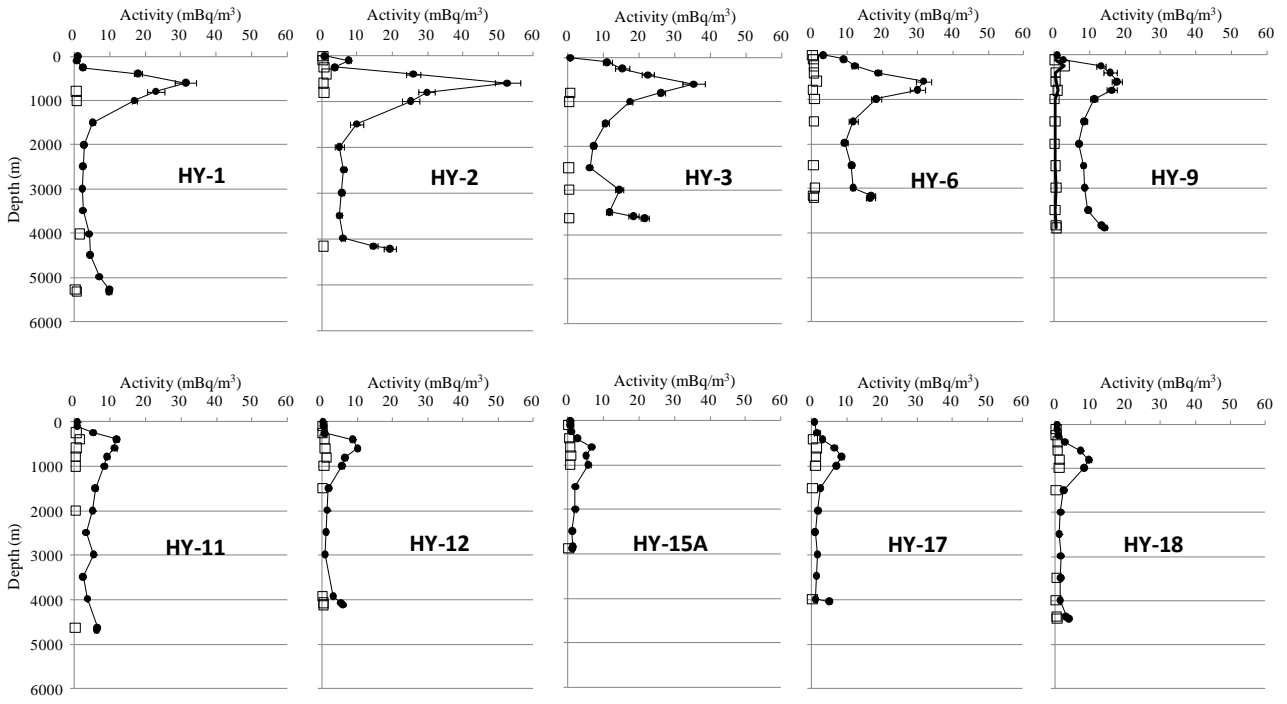


Fig. 3

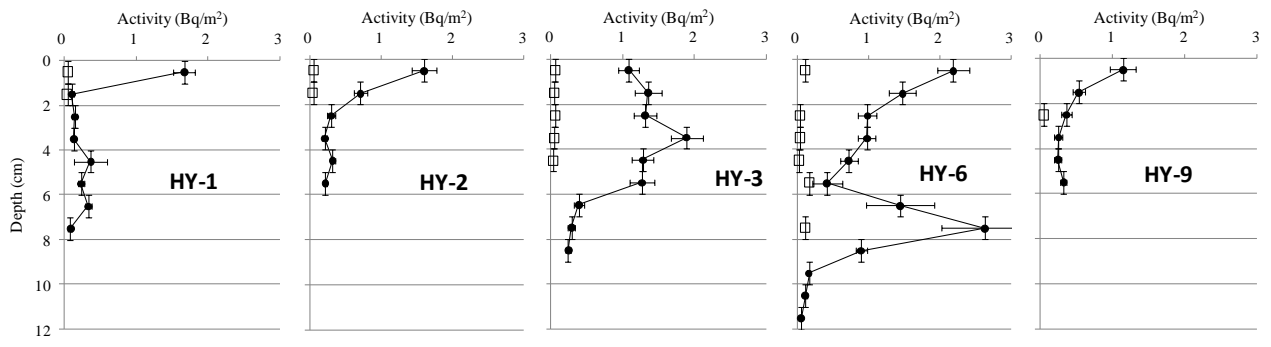


Fig. 4

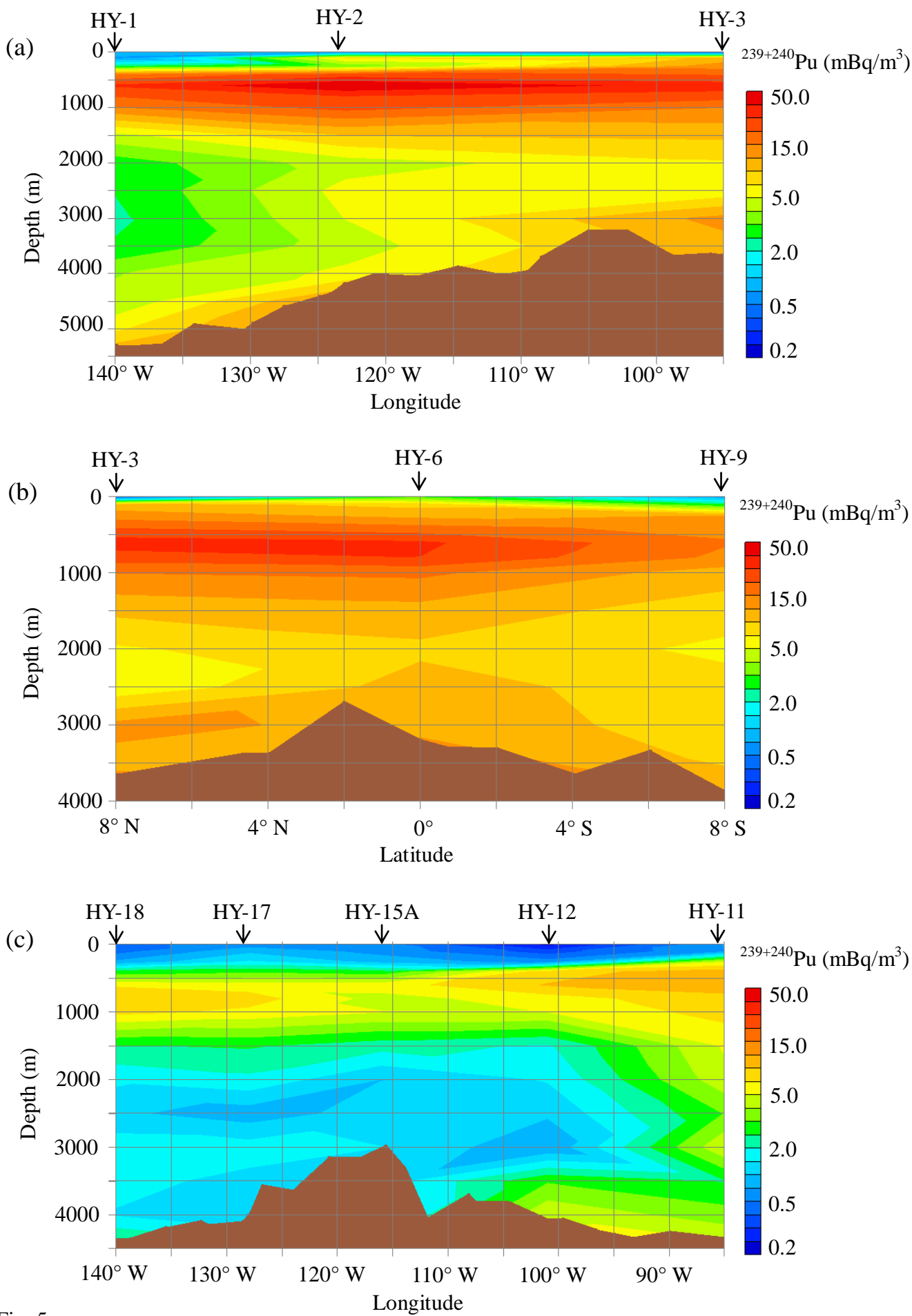


Fig. 5

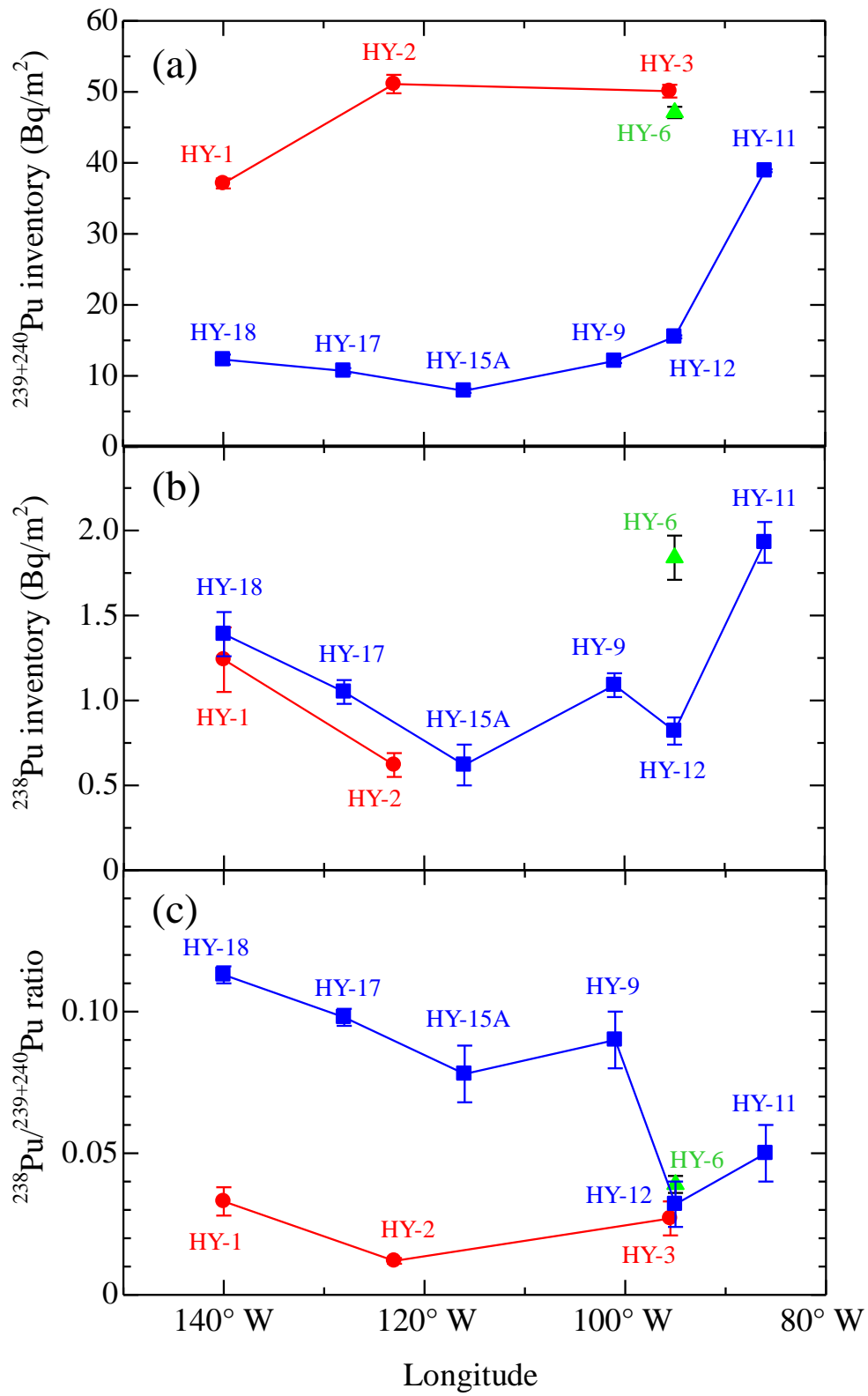


Fig. 6

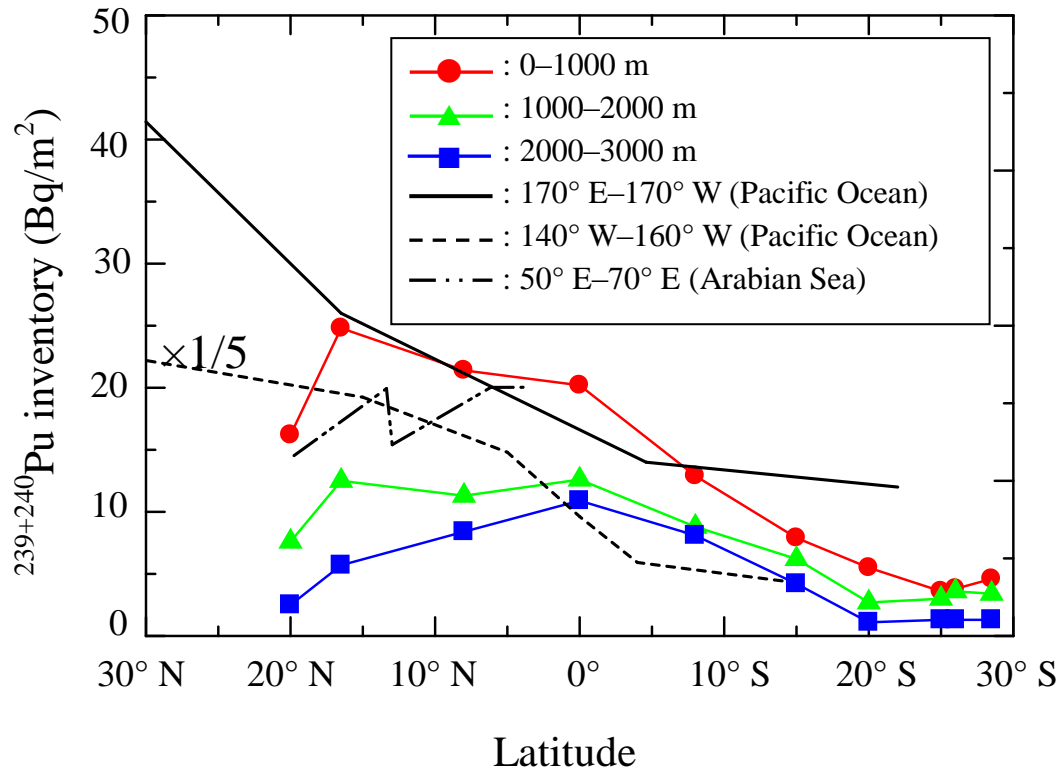


Fig. 7

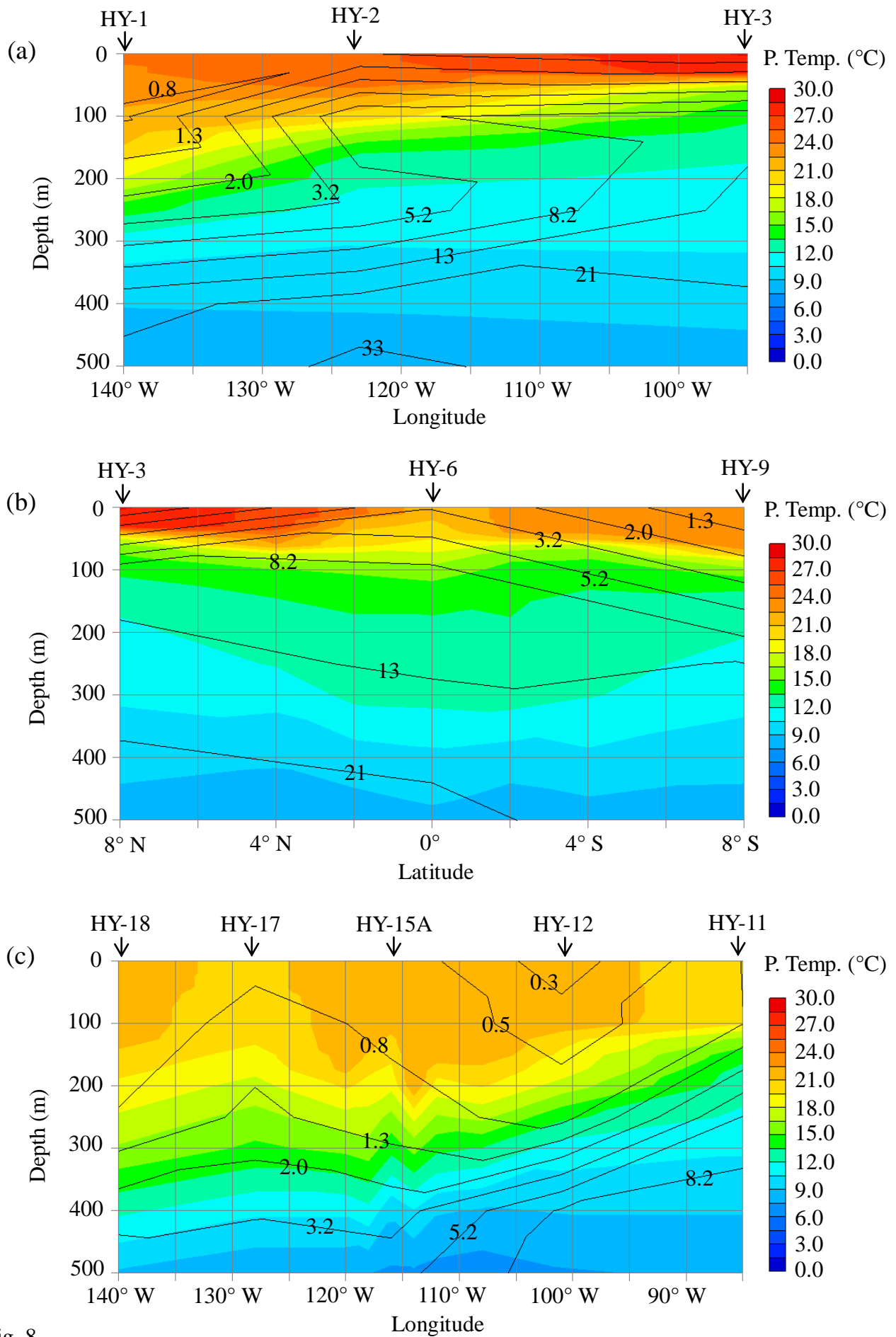


Fig. 8

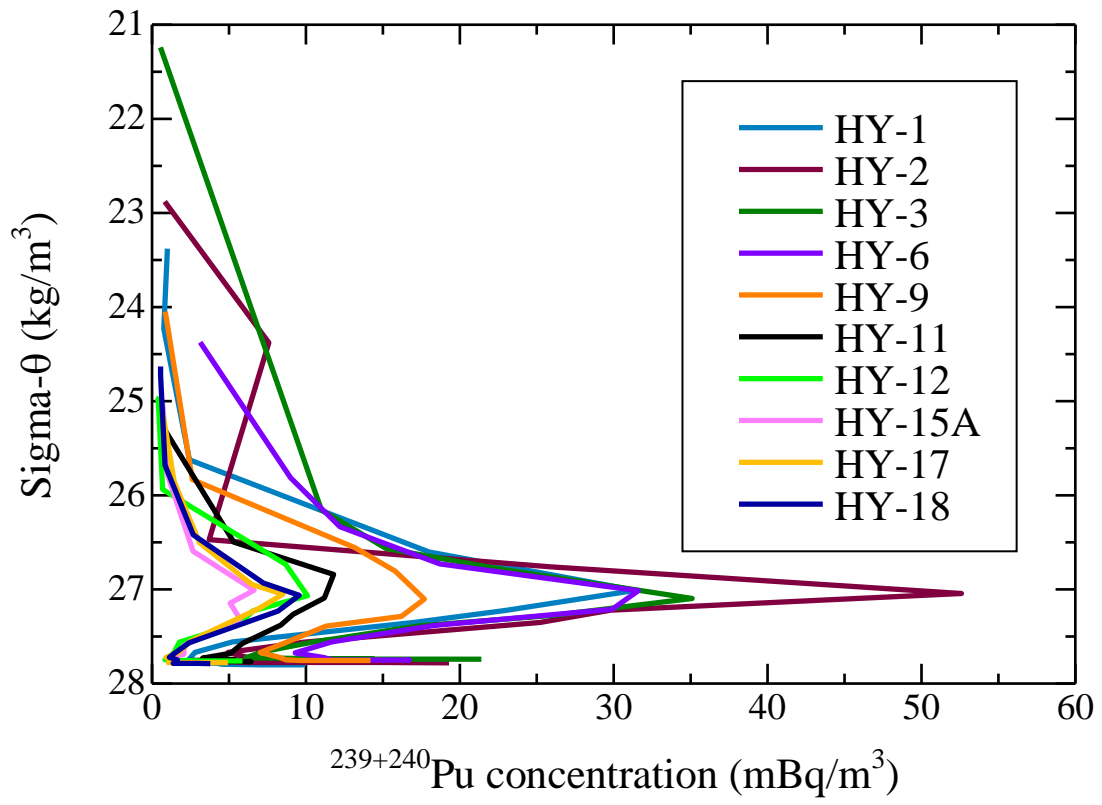


Fig. 9

